Journal of *Marine Science and Engineering*

MDPI

Article

Effects of Water Masses and Circulation on the Surface Water Partial Pressure of Carbon Dioxide in Summer in Eastern Beibu Gulf, China

Yu Ma [1,2], Tuanjie Li [3], Huayong Xia [4], Ruixiang Li [1,2], Yonggang Cao [1,2,*], Huaming Shi [1,2], Xin Xu [1,2], Jinshang Zhang [1,2], Weijie Zhang [1,2] and Xibao Su [1,2]

[1] South China Sea Marine Survey Center, Ministry of Natural Resources, Guangzhou 510275, China
[2] Key Laboratory of Marine Environmental Survey Technology and Application, Ministry of Natural Resources, Guangzhou 510300, China
[3] South China Sea Sea Area and Island Center, Ministry of Natural Resources, Guangzhou 510275, China
[4] South China Sea Marine Prediction Center, Ministry of Natural Resources, Guangzhou 510275, China
* Correspondence: caoyonggang@smst.gz.cn

Abstract: A gulf is a typical ecological zone where carbon cycle is jointly affected by complex environmental factors and strong human activities, and the Beibu Gulf has complex water masses and circulation structures. In this study, we used underway, continuous observational data of the surface water partial pressure of carbon dioxide (pCO_2), temperature (SST), salinity (SSS), dissolved oxygen (DO), and chlorophyll α along with vertical profile observations of temperature, salinity, carbonate system parameters and nutrients to determine the spatiotemporal variations and research effects of water masses and circulation on summer pCO_2 in the eastern part of Beibu Gulf. In the summers of 2011 and 2014, the mean pCO_2 in the eastern part of Beibu Gulf was 417 µatm and 405 µatm, respectively, and the mean sea–air CO_2 flux was 3.3 mmol m^{-2} d^{-1} and 1.6 mmol m^{-2} d^{-1}, respectively. In the summer of 2011, the northern part of the Beibu Gulf was controlled by a cyclonic circulation, and pCO_2 at the center of the cyclonic circulation increased by more than 15 µatm to a mean value of more than 10 µatm above that of the surrounding waters. The southern part of the Beibu Gulf was affected by an anticyclonic circulation and western coastal water masses, with a high temperature, low salinity, low pCO_2, and downwelling surface waters. In the summer of 2011, the mean pCO_2 was approximately 17 µatm lower than that in the surrounding waters, and no clear downwelling was observed in summer 2014. The eastern part of Beibu Gulf was a source of atmospheric CO_2 in the summer, only the region affected by the northern coastal water in the eastern part of Beibu Gulf was a sink of atmospheric CO_2, and pCO_2 had distinctly different spatiotemporal distributions under the influence of complex water masses and circulation structures.

Keywords: Beibu Gulf; partial pressure of carbon dioxide; controlling factor; water mass; circulation

Citation: Ma, Y.; Li, T.; Xia, H.; Li, R.; Cao, Y.; Shi, H.; Xu, X.; Zhang, J.; Zhang, W.; Su, X. Effects of Water Masses and Circulation on the Surface Water Partial Pressure of Carbon Dioxide in Summer in Eastern Beibu Gulf, China. *J. Mar. Sci. Eng.* **2023**, *11*, 46. https://doi.org/10.3390/jmse11010046

Academic Editor: Anatoly Gusev

Received: 3 December 2022
Revised: 23 December 2022
Accepted: 23 December 2022
Published: 29 December 2022

1. Introduction

Human activities have caused the concentration of atmospheric CO_2 to increase and exacerbate global climate change. The oceans have absorbed approximately 40% of the total CO_2 emitted by humans since the industrial revolution, thereby slowing the increase in atmospheric CO_2 concentration and temperature. Marginal seas only accounted for 7–8% of the global ocean area, but they played an important role in the global ocean carbon cycle and have been extensively studied by Cai (2011), Ikawa et al. (2011), Rysgaard et al. (2012) and Dixit et al. (2019) [1–4], among others. Continental-shelf marginal seas account for 12% of the total global marginal sea area and are essential in the carbon cycle of marginal seas [5–7]. The South China Sea (SCS) is one of the three largest marginal seas in the world. The carbon source/sink pattern of the SCS and biogeochemical processes have been studied by Chen et al. (2006), Chai et al. (2009), Zhai et al. (2013), and Ma et al. (2020) [8–11]. The

Beibu Gulf is the second largest gulf in the SCS, the components of water masses in the Beibu Gulf are complex, mainly including Qiongzhou Strait passage water, coastal water mass, SCS intrusion water, and mixed water masses (Figure 1) [12,13]. In summer, the circulation in the northern part of Beibu Gulf is cyclonic and that in the southern part is anticyclonic. There are interannual and monthly periodic oscillations (Figure 1) [14,15]. The complex water masses and circulation structures in the Beibu Gulf affect the biogeochemical processes of carbon and nutrients [16,17]. In this study, we used underway continuous observations and vertical profile observations to study spatiotemporal variations in the partial pressure of carbon dioxide in the surface water (pCO_2) in the Beibu Gulf in the summer and the corresponding controlling factors.

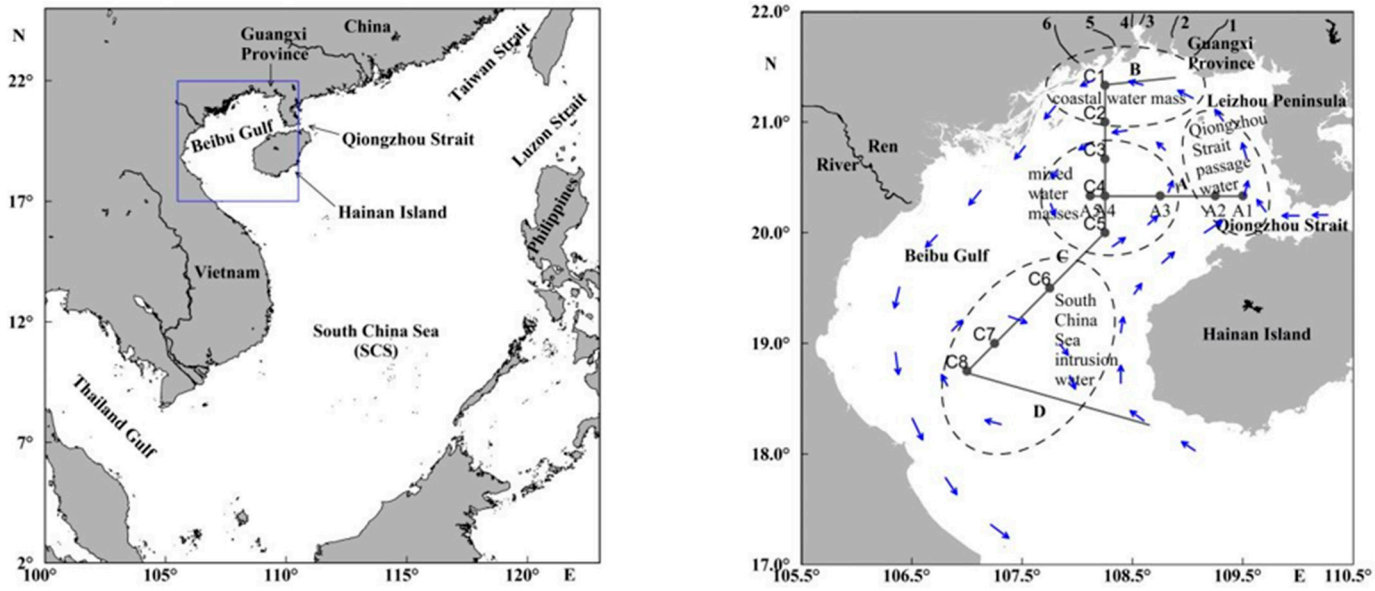

Figure 1. Map of the location of the Beibu Gulf, and transects, rivers on the Guangxi Province coast (1 Nanliu River, 2 Dafeng River, 3 Qin River, 4 Maoling River, 5 Fangcheng River and 6 Beilun River), water masses, circulation (blue arrows) in summer in the Beibu Gulf.

2. Materials and Methods

2.1. Studied Areas

The Beibu Gulf spans 105.50° E to 110.00° E and 17.00° N to 22.00° N (Figure 1) and has a subtropical maritime climate. The area of the gulf is approximately 12.9×10^4 km^2, and the water depth is between 20 m and 60 m, averaging approximately 38 m. In winter, a northeast monsoon prevails, while in summer, a southwest monsoon prevails. The rainy season is from April to October. The Beibu Gulf neighbors the Leizhou Peninsula to the east, Guangxi Province to the north, Vietnam to the west, and the SCS to the south, and connects to the northern part of the SCS through the Qiongzhou Strait. The rivers on the coast of Guangxi to the north and on the coast of Vietnam to the west carry terrestrial materials into the sea, forming a unique natural environment that consists of an estuarine ecosystem and a gulf ecosystem. In this study, two full-depth observation sections (sections A and C) and two underway observation sections (sections B and D) were deployed in the eastern part of Beibu Gulf, and five and eight observation stations were deployed in sections A and C, respectively (Figure 1).

2.2. Field Observations

The underway sea–air CO_2 continuous observation system (GO8050, General Oceanics, Miami, FL, USA) collected pCO_2 and atmospheric partial pressure of carbon dioxide (pCO_{2a}) data. We calibrated the observation system by using CO_2 standard gas (produced by the Chinese Academy of Meteorological Sciences, with an uncertainty of less than 0.3%). The water intake pump continuously extracted seawater samples from the monitoring well

and delivered them to the laboratory at a high flow rate. The difference between the water temperature in the water vapor equilibrator of the observation system and the original water temperature was less than 0.2 °C. The water vapor equilibrator pCO_2 was calculated using the saturated vapor pressure equation [18]; pCO_2 in the equilibrator was corrected to pCO_2 in situ temperatures using the empirical formula of Takahashi et al. (1993) [19]. The atmospheric sampling site was located at the top of the bow, and was isolated from pollution sources such as the ship's chimney and human activities. Eco-environmental elements were simultaneously measured and mutually calibrated by using a temperature and salinity sensor (SBE21, SEA-BIRD, Seattle, WA, USA), a dissolved oxygen (DO) sensor (Oxygen Optode 3835, Aanderaa Bergen, Norway), and a multi-parameter water quality meter (YSI6600, YSI, New York, NY, USA). Meteorological elements were observed by a shipborne automatic weather instrument (XZC5-1, NOTC, Tianjin, China).

Water temperature and salinity was measured at conductivity–temperature–depth stations during the full-depth observation. Seawater samples were collected simultaneously. Seawater samples for measuring dissolved inorganic carbon (DIC) and total alkalinity (TALK) were poured into 250 mL glass bottles with ground glass stoppers until full and stored at room temperature after the addition of 0.1% (v/v) saturated mercuric chloride solution. TALK and DIC in seawater was determined by using an open-cell titration and nondispersive infrared absorption, the uncertainties of TALK and DIC were less than 0.1%. The pH in the vertical profile was analyzed by a high precision pH meter; its uncertainty was 0.005. Nutrient samples were filtered on site and poured into 100 mL plastic bottles until full and stored in a frozen state. The sample analysis method was based on flow injection analysis, and its uncertainty was 5%.

2.3. Sea–Air CO_2 Flux Estimation

The sea–air CO_2 flux estimation equation is $F = k \times s \times \Delta pCO_2$, where $k = 0.27\ u^2\ (Sc/660)^{-0.5}$ [20] is the CO_2 gas transmission rate, u is the mean 10 m wind speed during the observation period, s is the solubility of CO_2 in seawater, and ΔpCO_2 is the sea–air CO_2 partial pressure difference, that is, pCO_2—pCO_{2a}. Negative F values indicate that the ocean absorbs CO_2 from the atmosphere, whereas positive F values indicate that the ocean releases CO_2 into the atmosphere.

3. Results and Discussions

3.1. Distributions of pCO_2 and Underway Environmental Factors

3.1.1. Spatiotemporal Distributions of pCO_2

In the summer of 2011, pCO_2 varied between 312 µatm and 522 µatm, with a mean of 417 µatm, pCO_{2a} was 375 µatm, and ΔpCO_2 was 42 µatm. In the summer of 2014, pCO_2 varied between 324 µatm and 527 µatm around a mean of 405 µatm, pCO_{2a} was 377 µatm, and $\triangle pCO_2$ was 28 µatm (Table 1). Both these ΔpCO_2 values were positive. The mean pCO_2 was higher in section A than in the other sections in both 2011 and 2014, at 434 µatm and 426 µatm, respectively. pCO_2 was the highest at the western entrance of the Qiongzhou Strait and in the region to the west of the Leizhou Peninsula (Table 1, Figure 2). In 2011 and 2014, pCO_2 was relatively high in section D, at 420 µatm and 412 µatm, respectively. pCO_2 gradually increased from the inner gulf to the mouth of the gulf (Table 1, Figure 2). The lowest mean pCO_2 of 400 µatm in 2011 and 370 µatm in 2014 occurred in section B. pCO_2 was the lowest in the intersection areas between sections B and C (Table 1, Figure 2). In addition, pCO_2 in section C between 20.5° N and 21.0° N in 2011 was higher than that in the surrounding areas; in 2011 and 2014, pCO_2 in the waters near 19.5° N in the southern part of section C was lower than that in the surrounding areas (Figure 2).

Table 1. Summary of pCO_2, SST, SSS, DO, chlorophyll *a* and sea–air CO_2 flux estimation in the summers of 2011 and 2014.

Survey Period /Domains	pCO_2 μatm	ΔpCO_2 μatm	SST °C	SSS	DO mg L^{-1}	Chlorophyll *a* μg L^{-1}	Sea–Air CO_2 Flux mmol m^{-2} d^{-1}
Summer 2011	312–522 417 ± 28	42	29.73–31.43 30.47 ± 0.38	29.77–33.17 31.98 ± 0.71	6.63–8.06 7.11 ± 0.08	0.1–6.4 0.5 ± 0.6	3.3 ± 2.8
A transect	390–522 434 ± 40	59	29.90–31.11 30.36 ± 0.35	31.53–32.60 32.19 ± 0.29	6.69–8.06 7.01 ± 0.10	0.3–4.4 0.6 ± 0.6	4.6 ± 2.8
B transect	312–485 400 ± 48	25	29.98–30.80 30.29 ± 0.25	29.76–31.22 30.31 ± 0.42	6.63–7.61 7.22 ± 0.14	0.7–4.6 1.6 ± 0.9	2.0 ± 6.0
C transect	313–437 411 ± 19	36	30.27–31.43 30.77 ± 0.30	29.93–32.77 32.00 ± 0.52	7.00–7.98 7.12 ± 0.07	0.3–0.7 0.3 ± 0.1	2.8 ± 1.4
D transect	409–439 420 ± 8	45	29.73–30.33 30.15 ± 0.13	31.67–33.17 32.48 ± 0.44	6.98–7.25 7.10 ± 0.03	0.3–0.6 0.3 ± 0.1	3.5 ± 0.3
Summer 2014	324–527 405 ± 42	28	29.03–31.44 29.97 ± 0.54	24.04–33.05 31.62 ± 1.89	6.58–7.41 7.07 ± 0.11	0.1–2.5 0.9 ± 0.5	1.6 ± 2.2
A transect	359–527 426 ± 66	49	29.61–31.44 30.31 ± 0.70	31.18–32.33 31.88 ± 0.38	6.60–7.23 6.99 ± 0.11	0.5–2.0 1.2 ± 0.3	2.8 ± 3.5
B transect	324–424 370 ± 24	−7	29.24–29.68 29.39 ± 0.09	24.04–26.31 25.13 ± 0.74	6.58–7.41 6.90 ± 0.13	0.9–2.1 1.4 ± 0.3	−0.4 ± 1.3
C transect	338–451 384 ± 21	7	29.03–30.19 29.78 ± 0.27	28.07–32.86 31.82 ± 1.03	6.59–7.33 7.12 ± 0.07	0.1–2.5 0.9 ± 0.5	0.4 ± 1.1
D transect	384–429 412 ± 13	35	29.29–30.43 29.75 ± 0.26	32.62–33.05 32.90 ± 0.11	7.20–7.38 7.28 ± 0.02	0.1–1.0 0.5 ± 0.2	2.0 ± 0.7

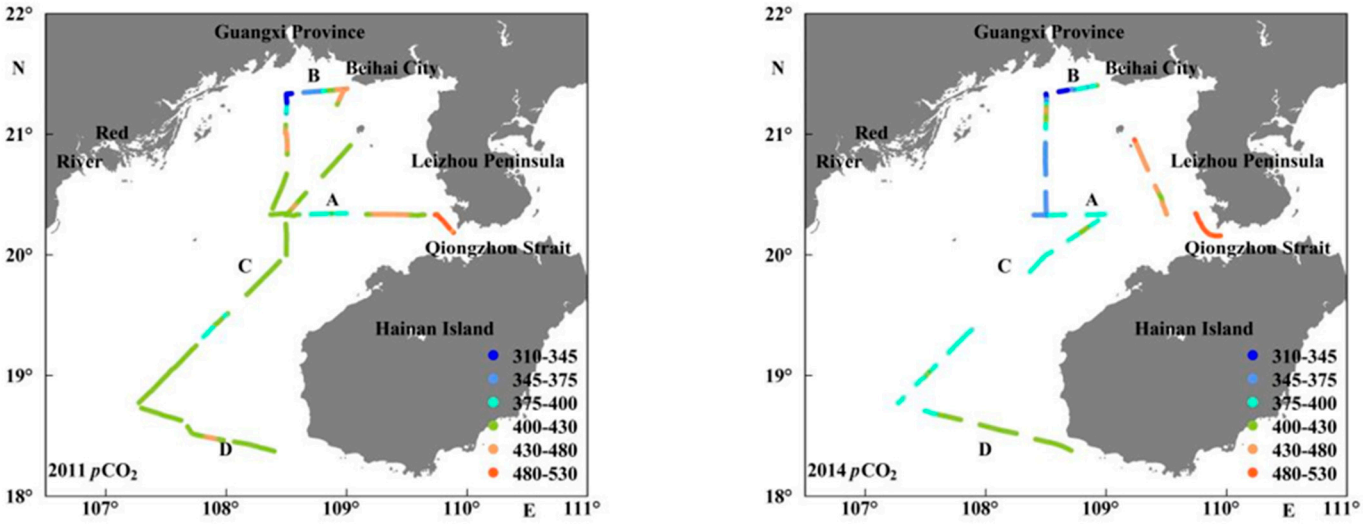

Figure 2. Spatiotemporal variations of pCO_2 in surface waters in the summers of 2011 (**left**) and 2014 (**right**).

3.1.2. Distributions of Underway Environmental Factors

The mean values of sea surface temperature (SST) were 30.47 °C and 29.97 °C in the summer of 2011 and 2014, respectively (Table 1). The high SST values in 2011 ranged from 30.27 to 31.43 °C around a mean of 30.77 °C (Table 1) and were distributed over the area at the northern end of section C near 21.0° N and at the southern end near 19.5° N. The middle part of the area was characterized by a low temperature (Figure 3). The high SST values in 2014 ranged from 29.61 to 31.44 °C around a mean of 30.31 °C (Table 1) and were located at the western entrance of the Qiongzhou Strait and to the west of the Leizhou Peninsula (Figure 3) in section A. During the observation period, the SST was low along sections B and D (Figure 3).

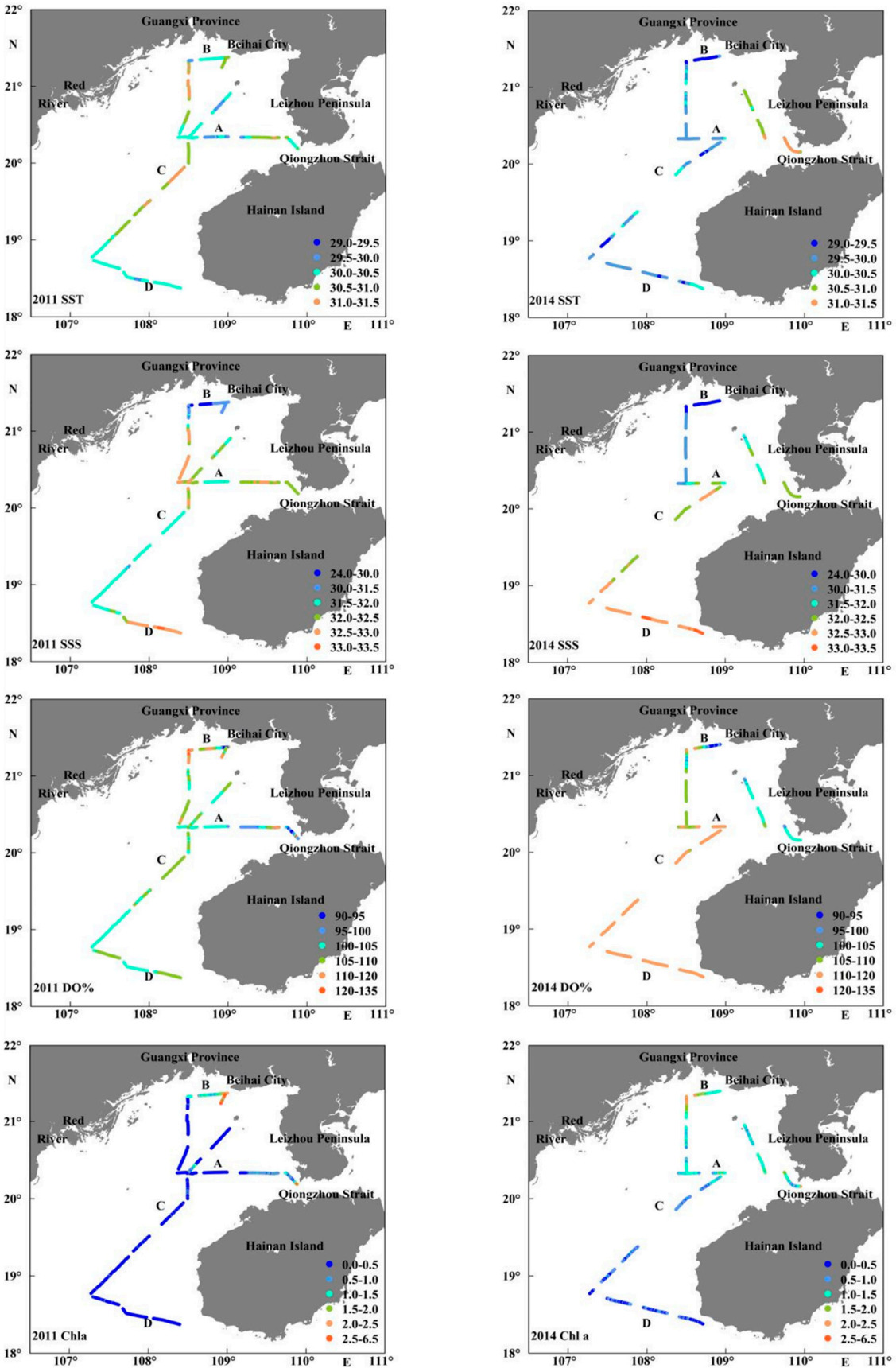

Figure 3. Spatiotemporal variations of SST, SSS, DO% and chlorophyll a in surface waters in the summers of 2011 (**left**) and 2014 (**right**).

The mean sea surface salinity (SSS) was 30.31 in 2011 and 25.13 in 2014. SSS in section B in 2014 was clearly lower than in 2011 and was distributed over a wider area (Table 1, Figure 3); the lowest SSS was in section B and ranged from 29.76 to 31.22 and from 24.04 to 26.31 in the summers of 2011 and 2014, respectively. In addition, there was a large area of low SSS in the southern part of section C in 2011 (Table 1, Figure 3). The low salinity of sections B and C was mainly affected by coastal water masses. The highest SSS in 2011 was between 20.5 and 21.0° N in section C (32.77) and in the waters east of 107.5° E in section D (33.17). The highest SSS in 2014 was in section D, with a maximum of 33.05 (Table 1, Figure 3). The high salinity feature of section D was controlled by SCS intrusion water.

The DO concentration in the eastern part of Beibu Gulf ranged from 6.63 mg L^{-1} to 8.06 mg L^{-1} and 6.58 mg L^{-1} to 7.41 mg L^{-1} in the summer of 2011 and 2014, respectively (Table 1). DO was high where sections B and C meet, but the highest value of DO in the summer of 2011 was more than that in the summer of 2014 (Figure 3). The distributions of high chlorophyll *a* was similar to that of DO, the maximum of chlorophyll *a* was 6.4 μg L^{-1} in the summer of 2011 and higher than 2.5 μg L^{-1} in the summer of 2014. In both 2011 and 2014, section B was a high chlorophyll *a* area [12,21]. However, the high chlorophyll *a* area in 2011 was located at the eastern end of section B, whereas chlorophyll *a* was highest in 2014 where sections B and C meet (Figure 3). The distribution area of highest DO and chlorophyll *a* was essentially consistent with the lowest pCO_2 (Figures 2 and 3).

3.2. Impact of Water Masses in Eastern Beibu Gulf on pCO_2

3.2.1. Qiongzhou Strait Passage Water

The direction of the Qiongzhou Strait transport is westward all year round. Water flows from the northern part of the SCS from the east to the west through the Qiongzhou Strait into the Beibu Gulf (Figure 1). At the western entrance of the Qiongzhou Strait, the flow turns northwestward and northward along the waters to the west of the Leizhou Peninsula. After reaching the coast of Guangxi Province, the flow turns westward (Figure 1) [22,23]. Under the influence of the Qiongzhou Strait passage water, pCO_2 at the western of the Qiongzhou Strait and in the waters to the west of the Leizhou Peninsula was relatively high (above 430 μatm) in the summers of 2011 and 2014 (Figure 2). The impact range could reach waters near 109 °E. Moreover, dissolved inorganic nitrogen (DIN) and phosphate (PO_4^{3-}) concentrations were high in the waters near the western entrance. The corresponding maximum values of these two variables were, respectively, 146.9 μg L^{-1} and 27.0 μg L^{-1} in the summer of 2011 and 121.4 μg L^{-1} and 8.2 μg L^{-1} in the summer of 2014. These nutrient concentrations, especially those of phosphate, were higher in 2011 than in 2014 (Figures 4 and 5). When the passage water reaches the western entrance, it diverges in the direction of the flow and slows. Sediment suspended in water precipitates and accumulates near the western entrance, leading to an increase in water transparency [24]. Nutrients carried by water promote phytoplankton growth, and photosynthesis absorbs CO_2 in water. In the summer of 2011, pCO_2 fell sharply in a small area at the western entrance of the Qiongzhou Strait to a minimum that was approximately 80 μatm lower than in the surrounding waters (Figure 2). In addition, in the summer of 2011, the upper water centered at 108.75 °E in section A had low temperature and low salinity (Figure 4), and pCO_2 ranged from 390 μatm to 400 μatm. The mean pCO_2 of 396 μatm was significantly lower than that of section A (434 μatm) (Figure 2). According to the sea-surface meteorological observation results, it was possible that heavy rainfall process diluted SSS and reduced SST and pCO_2, and that wind during the rainfall strengthened, which increased the upper mixed layer depth (Figures 2 and 3). In the summers of 2011 and 2014, the surface water at the western end of section A had a high temperature but low salinity (Figure 4), whereas the water temperature was low and the salinity was high at the bottom. The difference between the surface and bottom waters was obvious (Figures 3 and 4). The surface water is the coastal water mass from the western coast that is brought to the central and eastern parts under the combined effect of the monsoon and cyclonic circulation [25]. The bottom water is SCS

intrusion water from the southern mouth of the gulf. These characteristics of water masses will be analyzed later based on the observations for sections C and D.

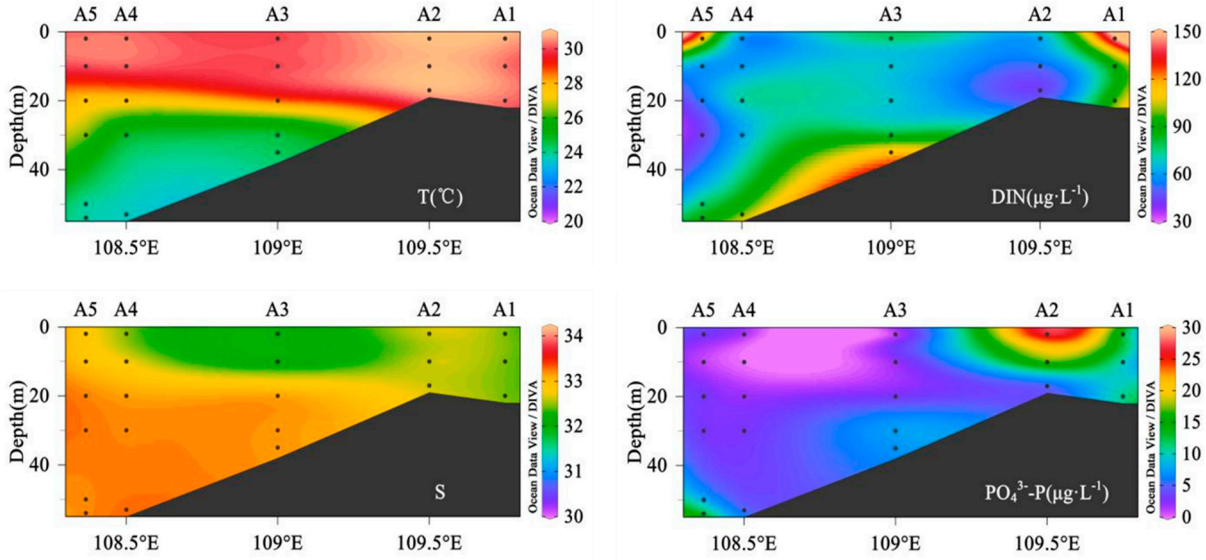

Figure 4. Distribution of temperature, salinity, DIN and PO_4^{3-} along A transect in the summer of 2011.

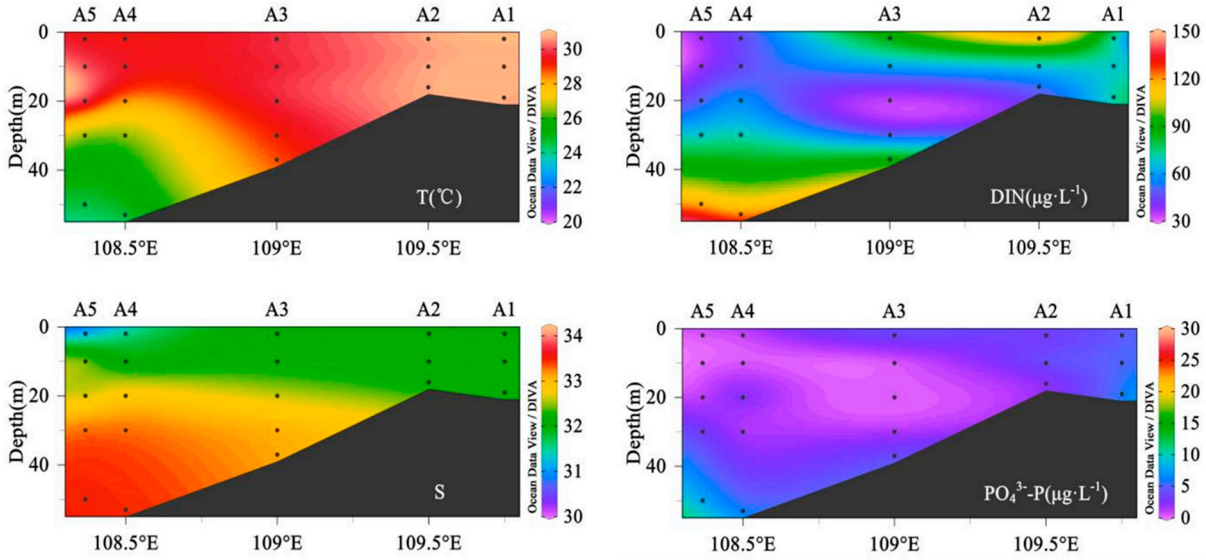

Figure 5. Distribution of temperature, salinity, DIN and PO_4^{3-} along A transect in the summer of 2014.

3.2.2. Coastal Water Mass

The northern coastal water mass of the Beibu Gulf is mainly composed of runoffs from the Nanliu River, Dafeng River, Qin River, Maoling River, Fangcheng River and Beilun River on the Guangxi coast (Figure 1), the salinity of this water mass is generally not greater than 32 [15]. The SSS in coastal water was lower than 31.5 in the summers of both 2011 and 2014; section B and the northern of section C were controlled by coastal water (Figure 3). The northern coastal water mass decreased the salinity while carrying nutrients that facilitated phytoplankton reproduction, but pCO_2 and SSS showed a negative correlation when SSS was less than ~ 27 (Figure 6). DIC was imported into the coastal area by runoff, while low water transparency limited the growth of phytoplankton. The concentration of chlorophyll *a* reached the maximum when SSS increased to ~ 27, phytoplankton photosynthesis absorbed CO_2 in water and released O_2, resulting in an increase in chlorophyll *a* and DO and a decrease in pCO_2 in section B (Figure 6). The minimum pCO_2 in section B in the summers of

2011 and 2014 was 312 µatm and 324 µatm, respectively (Table 1, Figure 2). pCO_2 and SSS showed a positive correlation when SSS was higher than ~ 27 (Figure 6), mainly because the concentration of chlorophyll *a* and DO% gradually decrease with the increase in SSS (Figures 2 and 3), and the role of phytoplankton in absorbing CO_2 in water decreased, leading to the gradual increase in pCO_2 (Figures 2 and 3). These results were consistent with the distribution characteristics of a typical estuarine plume area [26,27].

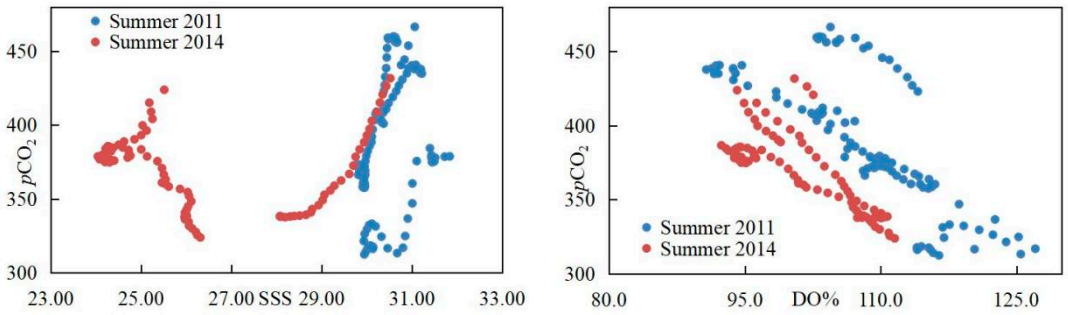

Figure 6. Relationships between pCO_2 and SSS, and between pCO_2 and DO% in coastal water.

The northern end of section C is also affected by the coastal water mass. In the summer of 2011, the northern coastal water mass was limited to the waters north of 21° N in section C, where the water depth of coastal water mass was approximately 10 m. This area has low TALK and DIC, with minimum values of 2011.0 µmol kg^{-1} and 1579.4 µmol kg^{-1}, respectively (Figure 7). In the summer of 2014, the northern coastal water arrived further south, at 20° N in the middle of section C, where the water depth of coastal water mass was approximately 20 m. There were relatively large areas of low TALK and DIC (Figure 8), with minimum values of 2022.0 µmol kg^{-1} and 1658.6 µmol kg^{-1}, respectively. There were temporal and spatial differences in the impact range of the northern coastal water mass. There was a low-SSS area in the northern Beibu Gulf in 2011 with a minimum SSS of 29.77 and a large low-SSS area in the central and northern waters in 2014, with a minimum SSS of 24.04 (Table 1, Figure 3). This indicated that the runoff into the sea in the summer of 2014 was greater than that in 2011; the coastal water might be from different runoffs since they had not been able to fully mix due to low flux into the sea (Figure 6). However, the clear upwelling of bottom water between 20° N and 21° N in the summer of 2011 also prohibited the coastal water mass from spreading further southward (Figure 7).

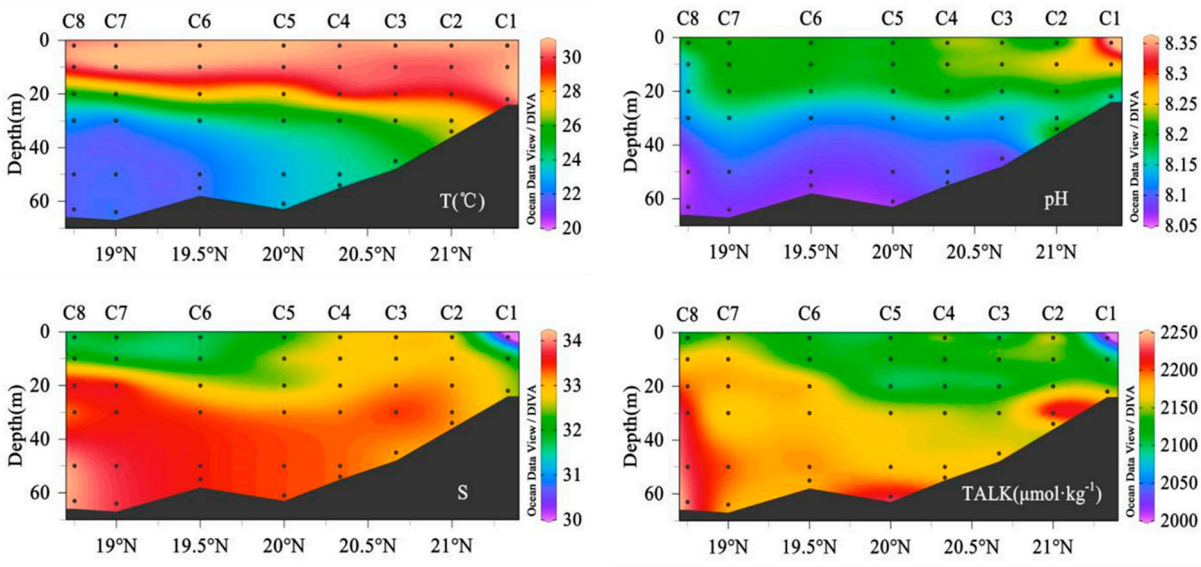

Figure 7. *Cont.*

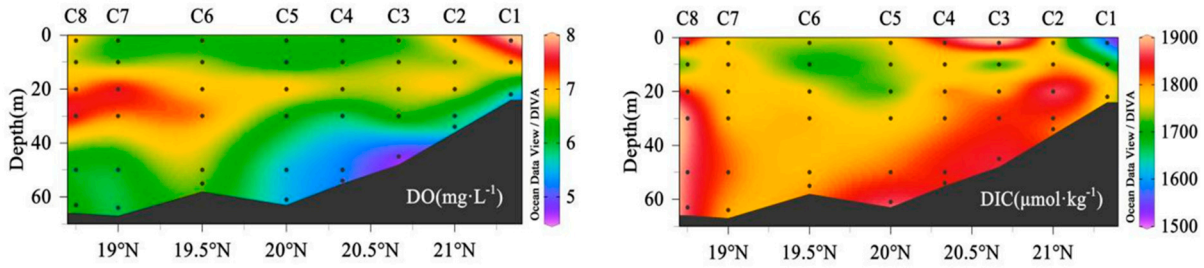

Figure 7. Distribution of temperature, salinity, DO, pH, TALK and DIC along the C transect in the summer of 2011.

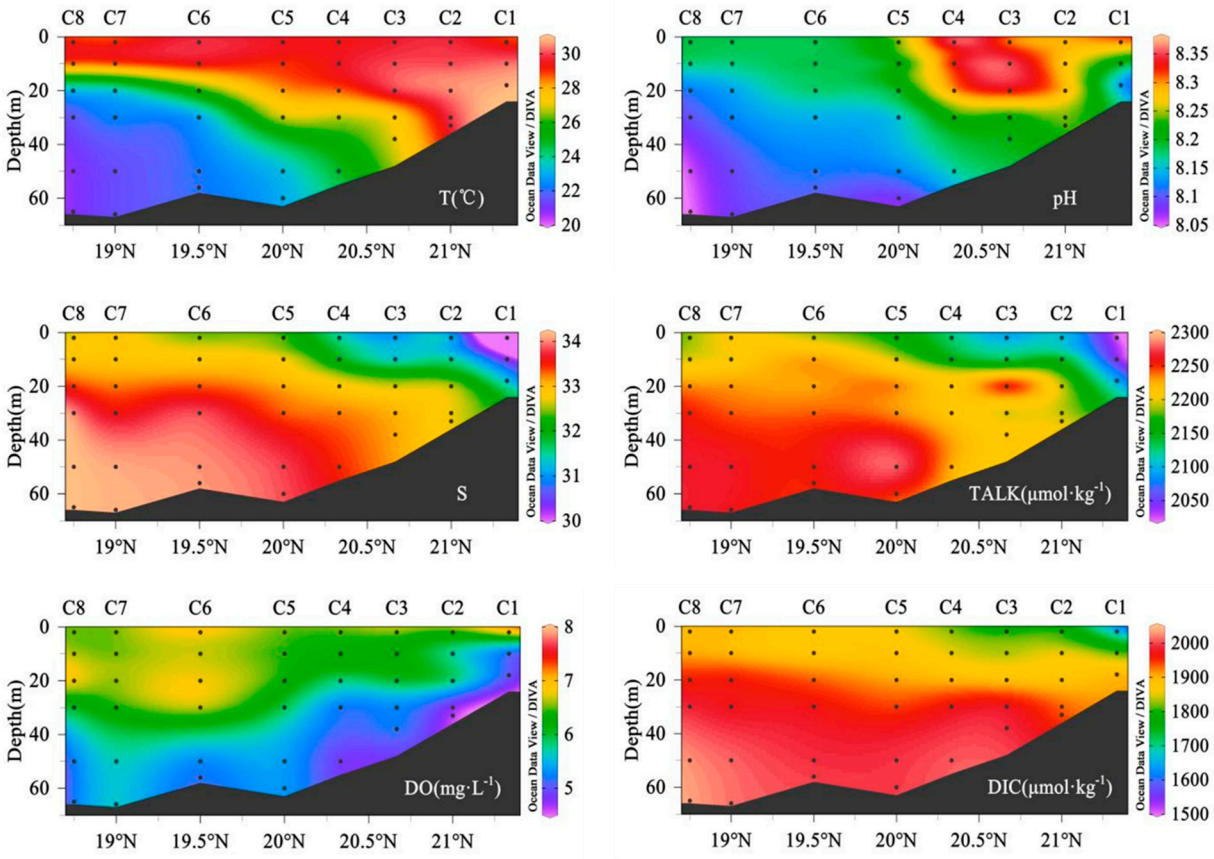

Figure 8. Distribution of temperature, salinity, DO, pH, TALK and DIC along the C transect in the summer of 2014 (Figures 4, 5, 7 and 8 are drawn by ODV [28]).

pCO_2 ranged from 431 µatm to 479 µatm, with a mean of 451 µatm. pCO_2 had extremely high values and DO% dropped at the eastern end of section B (Figure 6), although the high chlorophyll *a* area in the summer of 2011 was located at the eastern end of section B (Figure 3). This result was obtained mainly because the eastern end of section B is close to Beihai city, Guangxi Province. Due to the influence of urbanization there, the runoff into the sea promotes phytoplankton photosynthesis, while a large quantity of organic matter is also imported, and the degradation of organic matter and biological oxygen-consuming respiration increase pCO_2 in the water [29,30]. Moreover, the mangroves and salt marsh ecosystems along the coast had a certain contribution to the addition of pCO_2 [31].

3.2.3. SCS Intrusion Water

The surface and subsurface saline water (S = ~34.0) of the SCS intrudes into the Beibu Gulf from the southern mouth of the gulf (Figure 1). In some years, saline water can reach sea areas nearly as far north as 20.5° N [32]. In the summer of 2011, saline SCS intrusion

water reached areas near 19° N, and this water mass went beyond 20° N to near 20.25° N in the summer of 2014. There was more intense SCS water intrusion in the summer of 2014 than in 2011, but the bottom water between 20.5° N and 21.0° N upwelled in the summer of 2011 (Figures 7 and 8). Due to the influence of the SCS intrusion water, the DO and pH of the bottom water in section C showed a distinct decrease. The minimum DO of 4.79 mg L^{-1} and 4.65 mg L^{-1} in the summers of 2011 and 2014, respectively, was located near 20.5° N. The minimum pH of 8.07 and 8.05 for 2011 and 2014, respectively, was located in the southern most area of section C (Figures 7 and 8). The minimum DO of the bottom water in section C was located near 20.5° N. The reasons may be the following: (1) The water column in the eastern part of Beibu Gulf was obviously stratified in summer. As the DO-poor SCS intrusion water moved northward, the DO-rich surface water could not compensate for the low DO of the bottom layer. (2) When the range of influence of the SCS intrusion water reached 20.5° N, the combined effect of oxygen consumption by bottom organic matter (including terrestrial and marine organic matter) and biological respiration resulted in the low DO concentration at this location [33,34].

In the summer of 2011, the area in the southern mouth of the gulf with SSS greater than 33 was limited to the southeastern end of section D. In the summer of 2014, the areas with SSS greater than 33 reached 19° N, at the intersection between sections C and D (Figure 3). pCO_2 in areas with SSS higher than 33 in the southern mouth of the gulf was also greater than 400 µatm in the summers of 2011 and 2014 (Figures 2 and 3). pCO_2 and SSS gradually decreased from the southern mouth of the gulf to the inner gulf, and were positively correlated with SSS; SSS was a main controlling factor of pCO_2 (Figure 9). However, pCO_2 and DO% have no obvious correlation in the summer of 2011 when the intensity of SCS intrusion water was weak. pCO_2 was positively correlated with DO% in the summer of 2014, and DO% in DO-rich surface water gradually decreased, accompanied by a salinity reduction from the southern mouth of the gulf to the middle (Figure 9).

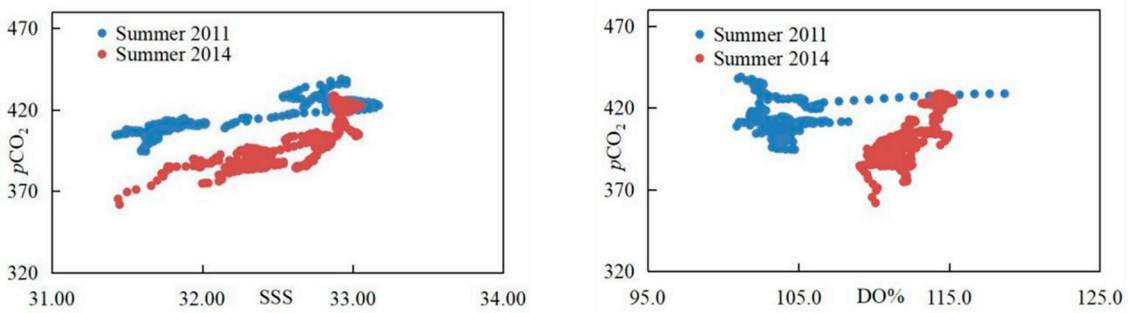

Figure 9. Relationships between pCO_2 and SSS, and between pCO_2 and DO% in sea area influenced by SCS intrusion water.

3.3. Impact of Circulation in Eastern Beibu Gulf on pCO_2

Ocean circulation is one of the most important factors that controls the absorption of anthropogenic CO_2 by the oceans. As a component of ocean circulation, coastal circulation has an important impact on seawater pCO_2 distribution and the ocean carbon source/sink pattern [35]. In summer, the northern part of the Beibu Gulf is controlled by a cyclonic circulation (Figure 1) [36,37]. During the summer observation in 2011, the circulation was centered between 20.5° N and 21.0° N in section C. The salinity of the entire water layer increased by approximately 1.0 and the temperature also decreased by about 0.5 °C in the center of cyclonic circulation, so the cyclonic circulation induced a clear upwelling of bottom water (Figure 7). As a result, DIC increased by approximately 100.0 µmol kg^{-1} (Figure 7), and pCO_2 ranged from 422 µatm to 437 µatm, with a mean of 432 µatm. Compared to the surrounding areas, pCO_2 at the circulation center was more than 15 µatm higher, and the mean was more than 10 µatm higher (Figure 2). The lowest DO in the bottom layer (4.79 mg L^{-1}) was between 20.5° N and 21.0° N in section C, and the pH was low (8.08). Upwelling-induced decreases in DO and pH are among the main factors causing ocean

hypoxia and acidification [38]. No significant upwelling of the bottom water was observed in the same area in the summer of 2014.

In the summer of 2011, in the area between 19° N and 20° N centered at 19.5° N in section C, the waters with high temperature and low salinity exhibited a clear downwelling tendency, and the vertical depth was greater than 20 m (Figure 7). pCO_2 ranged from 394 µatm to 405 µatm around a mean of 399 µatm, which was significantly lower than the mean pCO_2 of 416 µatm in the southern areas of section C (Figure 2). The DIC in the entire water layer was significantly reduced to below that of the surrounding area by approximately 100.0 µmol kg^{-1} (Figure 7). In the summer of 2014, SST was more or less the same area, but slightly increased, SSS decreased slightly, and pCO_2 was slightly lower than in the surrounding areas (Figure 2). No clear downwelling was observed in summer 2014 (Figure 8). In summer, the southern area of the Beibu Gulf is controlled by an anticyclonic circulation, and the surface water at the center of the circulation downwells (Figure 1) [37]. The observation results in section C between 19° N and 20° N were in line with the characteristics of anticyclonic circulation. The downwelling surface water of high SST and low SSS was from the Red River plume from Vietnam on the western coast of the gulf (the western coastal water mass), which spread offshore to the middle and eastern parts of the gulf [39]. Due to the impact of multiple factors, such as runoff and monsoon, there are interannual differences in the estuarine plume area [40]. The impact range of the western coastal water mass in the summer of 2011 was significantly greater than that in 2014 (Figures 2, 7 and 8).

3.4. Summer Sea–Air CO_2 Flux in Eastern Beibu Gulf

During the summer observation period in 2011 and 2014, the mean wind speed was 5.3 m s^{-1} and 4.6 m s^{-1}, respectively, and the sea–air CO_2 flux was 3.3 mmol m^{-2} d^{-1} and 1.6 mmol m^{-2} d^{-1}, respectively, corresponding to sources of atmospheric CO_2 (Table 1). These fluxes were comparable with the sea–air CO_2 fluxes of 3.2 mmol m^{-2} d^{-1} [41] and (1.9–3.8) mmol m^{-2} d^{-1} [42] that were reported in the waters over the continental slope in the northern SCS, whereas CO_2 fluxes above −0.2 mmol m^{-2} d^{-1} were reported in the shelf waters of the northern SCS [42]. In the summers of 2011 and 2014, the combined effect of coastal water masses and phytoplankton photosynthesis significantly reduced pCO_2 in the sea areas. The minimum pCO_2 was 312 µatm in 2011 and 324 µatm in 2014 (Table 1, Figure 2), corresponding to atmospheric CO_2 sinks. pCO_2 in coastal water affected by runoff input was mainly controlled by phytoplankton productivity or biological oxygen consumption respiration, and the coastal sea area acted as the sink of atmospheric CO_2 when phytoplankton productivity was stronger than biological oxygen consumption respiration [43,44].

The impact of the Qiongzhou Strait passage water and the SCS intrusion water mass resulted in relatively high pCO_2 in areas to the west of the Leizhou Peninsula and at the southern mouth of the gulf. In the summer of 2011, the sea–air CO_2 fluxes of sections A and D were 4.6 mmol m^{-2} d^{-1} and 3.5 mmol m^{-2} d^{-1}, respectively. In 2014, the sea–air CO_2 fluxes of sections A and D were 2.8 mmol m^{-2} d^{-1} and 2.0 mmol m^{-2} d^{-1}, respectively. This region was a source of atmospheric CO_2 in both years. In the middle of the gulf affected by the mixed water mass, pCO_2 was slightly lower. In the summers of 2011 and 2014, the sea–air CO_2 flux in section C was 2.8 mmol m^{-2} d^{-1} and 0.4 mmol m^{-2} d^{-1}, respectively. Moreover, offshore circulation caused an increase in pCO_2 at the cyclonic circulation center in the northern part of section C in the summer of 2011, and the CO_2 source intensity increased. Both pCO_2 and the CO_2 source intensity decreased at the center of the southern anticyclonic circulation. Section B was affected by coastal water masses and had the lowest pCO_2. The sea–air CO_2 fluxes in 2011 and 2014 were 2.0 mmol m^{-2} d^{-1} and −0.4 mmol m^{-2} d^{-1}, respectively. Section B remained a source of atmospheric CO_2 in 2011, mainly because the degradation of organic matter and biological oxygen-consuming respiration in the eastern area increased the water pCO_2.

4. Conclusions

1. In the summers of 2011 and 2014, pCO_2 in the eastern part of Beibu Gulf ranged from 312 µatm to 522 µatm and from 324 µatm to 527 µatm, respectively. The mean pCO_2 was 417 µatm and 405 µatm, pCO_{2a} was 375 µatm and 377 µatm, and the sea–air CO_2 fluxes were 3.3 mmol m^{-2} d^{-1} and 1.6 mmol m^{-2} d^{-1}, respectively. In both periods, the Beibu Gulf was a source of atmospheric CO_2.
2. The eastern part of Beibu Gulf was a source of atmospheric CO_2 in summer, only the region affected by the northern coastal water in the Beibu Gulf was a sink of atmospheric CO_2, and regions controlled by other water masses were sources of atmospheric CO_2. In the summer of 2011, the northern and southern parts of the Beibu Gulf were controlled by a cyclonic circulation and an anticyclonic circulation, respectively; pCO_2 at the circulation center was more than 15 µatm higher and approximately 17 µatm lower than in the surrounding areas.
3. The key ocean dynamical processes in the eastern part of Beibu Gulf have spatiotemporal differences, and the water masses and circulation structure are complex and variable. As a result, pCO_2 and sea–air CO_2 fluxes show characteristics of an uneven spatial distribution and interannual variability. Therefore, the carbon source/sink pattern and biogeochemical processes in the eastern part of Beibu Gulf need to be further studied.

Author Contributions: Conceptualization, investigation, data curation, Writing—review and editing, Y.M.; project administration and data curation, T.L.; conceptualization and formal analysis, H.X.; formal analysis and funding acquisition, R.L.; methodology and funding acquisition, Y.C.; Investigation and data curation, H.S.; Investigation and data curation, X.X.; visualization, J.Z.; Investigation, W.Z.; Investigation, X.S. All authors have read and agreed to the published version of the manuscript.

Funding: The study is supported by National Natural Science Foundation of China (Nos. 42174013); the National Key Research and Development Program of China under Grant (Nos. 2018YFB1802300) and the Sea Science&Technology Foundation of South China Sea Branch, Ministry of Natural Resources (Nos. 202205).

Institutional Review Board Statement: Not applicable.

Informed Consent Statement: Not applicable.

Data Availability Statement: Not applicable.

Conflicts of Interest: The authors declare no conflict of interest.

References

1. Cai, W. Estuarine and coastal ocean carbon paradox: CO_2 sinks or sites of terrestrial carbon incineration? *Annu. Rev. Mar. Sci.* **2011**, *3*, 123–145. [CrossRef] [PubMed]
2. Ikawa, H.; Oechel, W.C. Air-sea CO_2 exchange of beach and near-coastal waters of the Chukchi Sea near Barrow, Alaska. *Cont. Shelf Res.* **2011**, *31*, 1357–1364. [CrossRef]
3. Rysgaard, S.; Mortensen, J.; Juul-Pedersen, T.; Sørensen, L.L.; Lennert, K.; Søgaard, D.H.; Arendt, K.E.; Blicher, M.E.; Sejr, M.K.; Bendtsen, J. High air-sea CO_2 uptake rates in nearshore and shelf areas of Southern Greenland: Temporal and spatial variability. *Mar. Chem.* **2012**, *128–129*, 26–33. [CrossRef]
4. Dixit, A.; Lekshmi, K.; Bharti, R.; Mahanta, C. Net sea-air CO_2 fluxes and modeled partial pressure of CO_2 in open ocean of Bay of Bengal. *IEEE J. Sel. Top. Appl. Earth Obs. Remote Sens.* **2019**, *12*, 2462–2469. [CrossRef]
5. Dai, M.; Cao, Z.; Guo, X.; Zhai, W.; Liu, Z.; Yin, Z.; Xu, Y.; Gan, J.; Hu, J.; Du, C. Why are some marginal seas sources of atmospheric CO_2? *Geophys. Res. Lett.* **2013**, *40*, 2154–2158. [CrossRef]
6. Lohrenz, S.E.; Cai, W.; Chakraborty, S.; Huang, W.-J.; Guo, X.; He, Z.; Fennel, K.; Howden, S.; Tian, H. Satellite estimation of coastal pCO_2 and air-sea flux of carbon dioxide in the northern Gulf of Mexico. *Remote Sens. Environ.* **2018**, *207*, 71–83. [CrossRef]
7. Wanninkhof, R.; Triñanes, J.; Park, G.H.; Gledhill, D.; Olsen, A. Large decadal changes in air-sea CO_2 fluxes in the Caribbean Sea. *J. Geophys. Res. Oceans* **2019**, *124*, 6960–6982. [CrossRef]
8. Chen, C.T.A.; Wang, S.L.; Chou, W.C.; Sheu, D.D. Carbonate chemistry and projected future changes in pH and $CaCO_3$ saturation state of the South China Sea. *Mar. Chem.* **2006**, *101*, 277–305. [CrossRef]
9. Chai, F.; Liu, G.; Xue, H.; Shi, L.; Chao, Y.; Tseng, C.M.; Chou, W.C.; Liu, K.K. Seasonal and interannual variability of carbon cycle in South China Sea: A three-dimensional physical-biogeochemical modeling study. *J. Oceanogr.* **2009**, *65*, 703–720. [CrossRef]

10. Zhai, W.D.; Dai, M.H.; Chen, B.S.; Guo, X.H.; Li, Q.; Shang, S.L.; Zhang, C.Y.; Cai, W.J.; Wang, D.X. Seasonal variations of sea-air CO_2 fluxes in the largest tropical marginal sea (South China Sea) based on multiple-year underway measurements. *Biogeosciences* **2013**, *10*, 7775–7791. [CrossRef]
11. Ma, Y.; Shi, H.M.; Li, T.J.; Li, R.X.; Cai, Y.C.; Zhang, Y.; Xu, X.; Wang, X.; Wang, D. Spatiotemporal variations and controlling factors of the surface pCO_2 in the northern South China Sea. *IOP Conf. Ser. Earth Environ. Sci.* **2020**, *569*, 012092. [CrossRef]
12. Bauer, A.; Radziejewska, T.; Liang, K.; Kowalski, N.; Dellwig, O.; Bosselmann, K.; Stark, A.; Xia, Z.; Harff, J.; Böttcher, M.E.; et al. Regional differences of hydrographical and sedimentological properties in the Beibu Gulf, South China Sea. *J. Coast. Res.* **2013**, *66*, 49–71. [CrossRef] [PubMed]
13. Cao, Z.Y.; Bao, M.; Guan, W.B.; Chen, Q. Water-mass evolution and the seasonal change in northeast of the Beibu gulf, China. *Oceanol. Limnol. Sin.* **2019**, *50*, 532–542. (In Chinese)
14. Ding, Y.; Chen, C.; Beardsley, R.C.; Bao, X.; Shi, M.; Zhang, Y.; Lai, Z.; Li, R.; Lin, H.; Viet, N.T. Observational and model studies of the circulation in the Gulf of Tonkin, South China Sea. *J. Geophys. Res. Ocean.* **2013**, *118*, 6495–6510. [CrossRef]
15. Gao, J.; Xue, H.; Chai, F.; Shi, M. Modeling the circulation in the Gulf of Tonkin, South China Sea. *Ocean. Dyn.* **2013**, *63*, 979–993. [CrossRef]
16. Kaiser, D.; Unger, D.; Qiu, G. Particulate organic matter dynamics in coastal systems of the northern Beibu Gulf. *Cont. Shelf Res.* **2014**, *82*, 99–118. [CrossRef]
17. Lips, U.; Laanemets, J.; Lips, I.; Liblik, T.; Suhhova, I.; Suursaar, Ü. Wind-driven residual circulation and related oxygen and nutrient dynamics in the Gulf of Finland (Baltic Sea) in winter. *Estuar. Coast. Shelf Sci.* **2017**, *195*, 4–15. [CrossRef]
18. Weiss, R.F.; Price, R.A. Nitrous oxide solubility in water and seawater. *Mar. Chem.* **1980**, *8*, 347–359. [CrossRef]
19. Takahashi, T.; Olafsson, J.; Goddard, J.G.; Chipman, D.W.; Sutherland, S.C. Seasonal variation of CO_2 and nutrients in the high latitude surface oceans: A comparative study. *Glob. Biogeochem. Cycles* **1993**, *7*, 843–878. [CrossRef]
20. Sweeney, C.; Gloor, E.; Jacobson, A.R. Constraining global sea-air gas exchange for CO_2 with recent bomb ^{14}C measurements. *Glob. Biogeochem. Cycle* **2007**, *21*, GB2015. [CrossRef]
21. Tang, D.; Kawamura, H.; Lee, M.A.; Van Dien, T. Seasonal and spatial distribution of chlorophyll-a concentrations and water conditions in the Gulf of Tonkin, South China Sea. *Remote Sens. Environ.* **2003**, *85*, 475–483. [CrossRef]
22. Shi, M.; Chen, C.; Xu, Q.; Lin, H.; Liu, G.; Wang, H.; Wang, F.; Yan, J. The role of the Qiongzhou Strait in the seasonal variation of the South China Sea circulation. *J. Phys. Oceanogr.* **2002**, *32*, 103–121. [CrossRef]
23. Wu, D.; Wang, Y.; Lin, X.; Yang, J. On the mechanism of the cyclonic circulation in the Gulf of Tonkin in the summer. *J. Geophys. Res.* **2008**, *113*, C09029. [CrossRef]
24. Chen, B.; Xu, Z.; Ya, H.; Chen, X.; Xu, M. Impact of the water input from the eastern Qiongzhou Strait to the Beibu Gulf on Guangxi coastal circulation. *Acta Oceanol. Sin.* **2019**, *38*, 1–11. [CrossRef]
25. Minh, N.N.; Patrick, M.; Florent, L.; Sylvain, O.; Gildas, C.; Damien, A.; Van Uu, D. Tidal characteristics of the gulf of Tonkin. *Cont. Shelf Res.* **2014**, *91*, 37–56. [CrossRef]
26. Yin, K.; Harrison, P.J. Nitrogen over enrichment in subtropical Pearl River estuarine coastal waters: Possible causes and consequences. *Cont. Shelf Res.* **2008**, *28*, 1435–1442. [CrossRef]
27. Zhou, W.; Yin, K.; Harrison, P.J.; Lee, J.H. The influence of late summer typhoons and high river discharge on water quality in Hong Kong waters. *Estuar. Coast. Shelf Sci.* **2012**, *111*, 35–47. [CrossRef]
28. Michael Menzel, A.W.I.; Stephan Heckendorff, A.W.I. A new API for accessing ODV data collections from C++ and Java. *Boll. Geofísica* **2013**, *54*, 208.
29. Zhai, W.; Dai, M.; Guo, X. Carbonate system and CO_2 degassing fluxes in the inner estuary of Changjiang (Yangtze) River, China. *Mar. Chem.* **2007**, *107*, 342–356. [CrossRef]
30. Dai, J.; Zhang, X.; Wang, D.; Guo, C.; Fang, R.; Wang, X. Water quality change of Nanliu River in Guangxi Beibu Gulf Economic Zone. In Proceedings of the 2011 International Conference on Remote Sensing, Environment and Transportation Engineering, Nanjing, China, 24–26 June 2011; pp. 5629–5632.
31. Wang, Z.A.; Cai, W.J. Carbon dioxide degassing and inorganic carbon export from a marsh-dominated estuary (the Duplin River): A marsh CO_2 pump. *Limnol. Oceanogr.* **2004**, *49*, 341–354. [CrossRef]
32. Chen, L. *Study on Trophic Structure of the Beibu Gulf Ecosystem Using EwE Model*; Xiamen University: Xiamen, China, 2015; pp. 2–3. (In Chinese)
33. He, B.; Dai, M.; Zhai, W.; Guo, X.; Wang, L. Hypoxia in the upper reaches of the Pearl River Estuary and its maintenance mechanisms: A synthesis based on multiple year observations during 2000–2008. *Mar. Chem.* **2014**, *167*, 13–24. [CrossRef]
34. Li, X.L.; Shi, H.M.; Xia, H.Y.; Zhou, Y.P.; Qiu, Y.W. Seasonal hypoxia and its potential forming mechanisms in the Mirs Bay, the northern South China Sea. *Cont. Shelf Res.* **2014**, *80*, 1–7. [CrossRef]
35. Sarmiento, J.L.; Orr, J.C.; Siegenthaler, U. A perturbation simulation of CO_2 uptake in all ocean general circulation model. *J. Geophys. Res.* **1992**, *97*, 3621–3645. [CrossRef]
36. Xia, H.; Li, S.; Shi, M. Three-D numerical simulation of wind-driven currents in the Beibu Gulf. *Acta Oceanol. Sin.* **2001**, *23*, 11–23.
37. Gao, J.; Chen, B.; Shi, M. Summer circulation structure and formation mechanism in the Beibu Gulf. *Sci. China Earth Sci.* **2015**, *58*, 286–299. [CrossRef]
38. Wei, Q.S.; Yu, Z.G.; Xia, C.S.; Zang, J.Y.; Ran, X.B.; Zhang, X.L. A preliminary analysis on the dynamic characteristics of the hypoxiczone adjacent to the Changjiang Estuary in summer. *Acta Oceanol. Sinca* **2011**, *33*, 100–109.

39. Rogowski, P.; Zavala-Garay, J.; Shearman, K.; Terrill, E.; Wilkin, J.; Lam, T.H. Air-sea-land forcing in the Gulf of Tonkin: Assessing seasonal variability using modern tools. *Oceanography* **2019**, *32*, 150–161. [CrossRef]
40. Tong, G.; Chen, L.; Long, J.; Li, T.; Xiao, X.; Tong, S. Surface pollen distribution patterns in Beibu Gulf and corresponding sediment dynamics environment. *Chin. Sci. Bull.* **2012**, *57*, 902–911. [CrossRef]
41. Zhai, W.; Dai, M.; Cai, W.J.; Wang, Y.; Hong, H. The partial pressure of carbon dioxide and air-sea fluxes in the northern South China Sea in spring, summer and autumn. *Mar. Chem.* **2005**, *96*, 87–97. [CrossRef]
42. Li, Q.; Guo, X.; Zhai, W.; Xu, Y.; Dai, M. Partial pressure of CO_2 and air-sea CO_2 fluxes in the South China Sea: Synthesis of an 18-year dataset. *Prog. Oceanogr.* **2020**, *182*, 102272. [CrossRef]
43. Algesten, G.; Wikner, J.; Sobek, S.; Tranvik, L.J.; Jansson, M. Seasonal variation of CO_2 saturation in the Gulf of Bothnia indications of marine net heterotrophy. *Glob. Biogeochem. Cycles* **2004**, *18*, GB4021. [CrossRef]
44. Lefèvre, N. Low CO_2 concentrations in the Gulf of Guinea during the upwelling season in 2006. *Mar. Chem.* **2009**, *113*, 93–101. [CrossRef]